

Improvement of sensitivity and signal-to-noise ratio in a laser spectrophotometer with a 30-m long absorption cell

Yu.N. Ponomarev and I.S. Tyryshkin

*Institute of Atmospheric Optics,
Siberian Branch of the Russian Academy of Sciences, Tomsk*

Received September 9, 2003

An enhanced laser spectrophotometer with a 30-m long absorption cell and an alexandrite narrow-band tunable pulsed laser is described. The performance characteristics of modified alignment units for mirrors of a multipass optical system and a system for measurement of the amplitude ratio of pulsed signals from a photodetector are presented. As a result, the optical path length was extended from 1800 m to 2400 m and the experimental uncertainty in the transmission spectrum was reduced from 1% to 0.2%.

Introduction

Tunable pulsed visible and near-IR lasers, such as ruby, alexandrite, Ti:sapphire, and dye lasers are rather widely used in differential absorption and scattering (DIAL) lidars for sensing, for example, moisture profiles. Absorption lines of H₂O molecule in the short-wave spectral region are weak. The absorption coefficients at the peaks of lines used as reference ones usually do not exceed $5 \cdot 10^{-6} \text{ cm}^{-1} \cdot \text{atm}^{-1}$. The parameters of such weak absorption lines, namely, line intensity and halfwidth, air pressure induced shift, and the coefficients of the temperature dependence, should be measured accurate to 1–2% to suit the retrieval of the H₂O concentration along the sensing path with the error ~ 5 –10%. It is worth conducting such measurements with the same laser source as in the DIAL system to automatically take into account the effect of the shape and width of the laser line on the absorption spectrum recorded.

Laser spectrometers with long absorption cells^{1–3} equipped with multipass optical systems giving the total optical path length from hundreds meters to several kilometers provide for most accurate measurements of the line intensities. One of such spectrometers¹ is designed for precision measurements of the absolute values of the absorption coefficients of H₂O, O₂, and other molecules in the spectral range including the emission bands of the ruby, alexandrite, and Ti:sapphire lasers, that is, in some ranges from 690 to 780 nm. Use of a standard instrumentation for measuring the intensity ratio of radiation at the entrance into the absorption cell and at the exit from it (pulsed photodetectors, pulsed voltmeters with the 1–5% error of measuring the amplitude of a pulsed electric signals) allows determination of the absorption coefficient at a given wavelength of the laser pulse with the uncertainty up to $5 \cdot 10^{-8} \text{ cm}^{-1}$ (Ref. 1), which corresponds to $\Delta k/k = 10^{-2}$ (or $\Delta D/D$), where k is the absorption coefficient, in cm^{-1} ; D is the optical thickness of the absorbing layer at $k = 5 \cdot 10^{-6} \text{ cm}^{-1}$.

However, nowadays the use of the novel instrumentation for measurement of pulsed signals^{4–6} provides, in principle the possibility of measuring the optical thickness of the absorbing layer D even for the pulsed sounding radiation at the level of $\Delta D/D \sim 10^{-3}$ – 10^{-4} (Ref. 5).

In this paper we describe a modified spectrometer with a 30-m long absorption cell and an alexandrite tunable narrow-band pulsed laser. In this spectrometer, both the multipass optical system and the system for measurement of the amplitude ratio of pulsed signals recorded with a photodetector at the entrance in and exit from the absorption cell are enhanced. The H₂O and O₂ spectra recorded using a standard and the modified version of the spectrometer are analyzed.

Description of the spectrophotometer and the measurement and signal processing procedures

The functional diagram of the spectrometer is shown in Fig. 1.

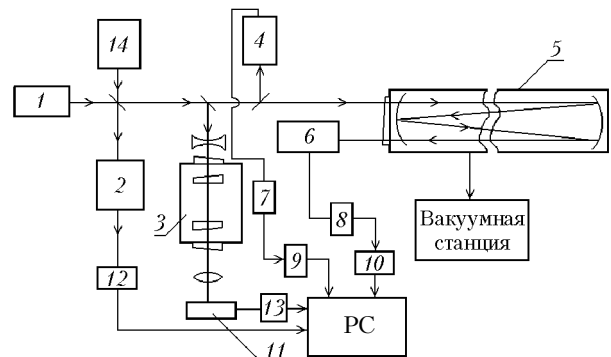


Fig. 1. Block diagram of the spectrophotometer.

The radiation of the alexandrite laser 1 is directed with beam splitters to the meters of radiation wavelength and the spectrum width 2 and 3 and to

the reference photodetector 4, then transmitted through the optical system of the multipass gas cell (MGC) 5, and received by the measuring photodetector 6. Photocells of the F-32 type are used as photodetectors. The signals from the photocells are recorded with a V4-17 pulsed voltmeters 7 and 8 and then entered into a PC through an ADC 9 and 10. For rough measurement of the radiation wavelength we use a commercial Spektron IV wave meter 2 including four vacuumized Fizeau interferometers with the spacing from 0.005 to 40 mm.

More accurate measurements of the wavelength and spectrum width are conducted using a vacuumized Fabry–Perot interferometer 3 with the spacing of 80 mm. The interference pattern at the interferometer output is recorded with a linear CCD array 11. The signals from Spektron IV and the linear CCD array are entered into a PC through an ADC 12, 13.

Specifications of the spectrometer are tabulated below.

Parameters	Before modernization	After modernization
MGC		
length, m	30	30
diameter, m	1.1	1.1
pressure, mm Hg	$5 \cdot 10^{-5} - 10^3$	$5 \cdot 10^{-5} - 10^3$
temperature, K	288–350	288–350
optical path length, m	60–1800	60–2400
laser		
tuning range, nm	720–780	720–780
spectrum width, cm^{-1}	$< 5 \cdot 10^{-3}$	$< 5 \cdot 10^{-3}$
tuning step	$\geq 5 \cdot 10^{-3}$	$\geq 5 \cdot 10^{-3}$
pulse repetition frequency, Hz	≤ 0.5	≤ 0.5
pulse duration, s	$\geq 180 \cdot 10^{-9}$	$\geq 180 \cdot 10^{-9}$
output pulse energy, J	$\geq 10^{-3}$	$\geq 10^{-3}$
recording system		
error in determination of line positions, cm^{-1}	$\leq 5 \cdot 10^{-3}$	$\leq 5 \cdot 10^{-3}$
error in measurement of gas cell transmittance, %	≤ 1	≤ 0.2
error in pressure measurement, mm Hg	≤ 0.1	≤ 0.1
threshold sensitivity, cm^{-1}	$5 \cdot 10^{-8}$	10^{-8}

The transmittance of the layer of a gas under study is determined by the equation

$$T_\lambda = (U_\lambda^{\text{out}}/U_\lambda^{\text{in}})/(U_{0\lambda}^{\text{out}}/U_{0\lambda}^{\text{in}}), \quad (1)$$

where U denotes the photodetector signals, the superscripts “in” and “out” correspond to U values at the entrance into the cell and the exit from it, the subscript 0 stands for U values obtained in the cell evacuated down to the pressure of $5 \cdot 10^{-5}$ mm Hg.

The absorption coefficient is determined from Eq. (1) using the Bouguer law:

$$T_\lambda = e^{k_\lambda L}, \quad (2)$$

where L is the length of the optical path in the multipass cell.

The water vapor absorption spectra recorded by the spectrometer before modernization were reported in Ref. 7. The error in determination of the intensities of relatively strong absorption lines is usually within 5%. Because of the difficulties connected with the increase of the optical path length for the radiation in the cell, the error in measurement of weak lines is much higher.

Modernization of the spectrometer described above was aimed at the increase in the length of the optical path by improving the long-term stability of the multipass optical system of the cell and the accuracy in measuring the amplitude of the signals recorded by the reference and sensing photodetectors.

Improvement of the stability of multipass optical system

Prior to modernization, each mirror holder of the Barskaya three-mirror optical system⁸ in the spectrometer was set on a movable table, which could be moved manually along two perpendicular directions from outside using the system of rods, cog-wheels, vacuum seals, and a worm gear. Such a mirror support and control system provided for relatively stable operation at the optical path length up to 1800 m at the objective mirrors of 15 cm in diameter and a 20×30 cm collective mirror.

With the increase of the optical path length, the separation between raster points on the collective mirror becomes comparable with the diameter of the sensing beam. The system misalignment due to temperature variations and vibrations may lead to beam vignetting by the system elements, and, consequently, to sharp increase of the errors in the transmission measurements.

To avoid this problem, we have developed remotely controlled, aligned mirror units with the electromechanical drives that are characterized by minimum free play. A new alignment unit (Fig. 2) operates as follows: a plate 2 with a leaf spring 3 fixed to it is rigidly mounted on a base 1. A spacer plate 4 is mounted to the spring. The mirror 6 is fixed on a plate 5, which is mounted to the spacer plate 4 with a spring. The spring deformation and the corresponding deflection of the mirror in the horizontal and vertical planes is performed by a microscrew 7 controlled by a stepper motor 8. The stepper motor and microscrew are housed in a sealed housing, and they operate at the atmospheric pressure. The plate is controlled through a bellows, while the microscrews are controlled by a DSh 78-0.16-1 stepper motors. A specially developed power supply units provide for both step-by-step and continuous rotation of the microscrew. The unit is controlled from a control panel, which can be connected to the cell ends through specialized connectors.

The stability of the old, not modernized, and the new optical-mechanical systems was tested in the following way. A beam from a continuous-wave He–Ne laser used for the alignment was passed through a

multipass optical system and directed to a two-coordinate linear array. To create vibrations near the alignment unit, a fore pump was put on the floor without dampers. As the pump was turned on, in the not modernized version we observed vertical blurring of the exit laser beam by up to 5 mm.

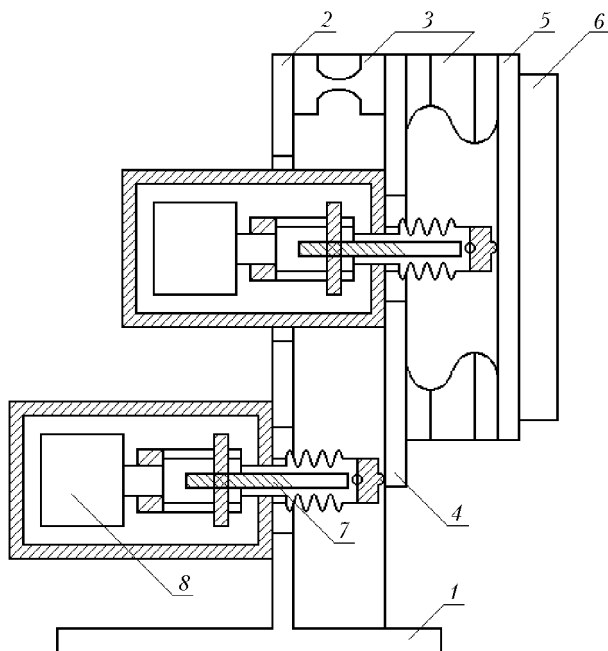


Fig. 2. Alignment unit.

With the new alignment units, we observed almost no deviation or blurring of the exit laser beam at both vibrations of the cell base and room temperature variation by $\sim 10^{\circ}\text{C}$. Once the alignment units were replaced, the optical path length, at which measurement stability was ensured, increased from 1800 to 2400 m.

Modernization of the meter of amplitude of signals from a photodetector

A two-channel meter of the amplitude of electric pulses recorded with a reference and output photodetectors with the data input into the computer was developed to replace the pulsed voltmeters used earlier. The blockdiagram of this meter is shown in Fig. 3.

Each of the channels of the meter of pulse amplitude consists of a unit for peak detection 3, matching amplifier 1, and an ADC 2. The unit for peak detection is designed to generate an ADC startup pulse when the input pulse achieves its peak value. This unit is a peak detector, in which the input pulse is normalized and then sent to a charging cascade responsible for charging a capacitor. The ADC converts the pulse amplitude into a digital binary 12-bit code. We use a MAXIM single-chip 12-

bit ADC with a built-in boxcar integrating detector that ensures the needed conversion accuracy.

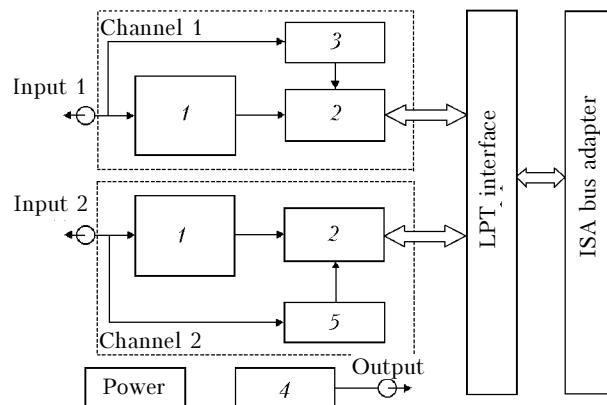


Fig. 3. Two-channel meter of electric pulse amplitude.

An interface serves for ADC coding, formation and transmission of the control signals from a PC, as well as for input of digital data into the PC.

A calibrator 4 serves as a source of stabilized voltage to check the working capacity of both of the ADC channels in the off-line mode. The matching amplifier is responsible for matching the high output photodetector resistance with a relatively low input ADC resistance.

The specialized software allows operating the meter (calibration, data input and storage) and provides for real-time display of the data in both digital and graphical form for a preliminary data processing.

The meter was tested during operation of the spectrometer with the pulsed alexandrite laser, whose characteristics are given in the Table. A signal from a single photodetector was applied to the input of both channels of the meter to avoid the errors caused by different photodetector characteristics. The tests have shown that at the amplitude variations of the photodetector output signal from 0.1 to 4 V, the error of measuring the ratio of the signals from the first and second channels did not exceed 10^{-3} .

The spectrometer characteristics that were achieved after modernization of its basic units are presented in the second column of the Table.

Figure 4 depicts an example of an absorption line profile recorded by the modernized spectrometer in comparison with the calculated Doppler profile. The spectrum was recorded at the water vapor pressure of about 1 mm Hg and the optical path length of 2000.64 m (68 passes of radiation through the cell). The obtained experimental values of the absorption coefficient were fit to the Doppler profile by the least-squares method. The bottom curve in Fig. 4 corresponds to the 50-time magnified difference between the calculated and experimental points. As follows from Fig. 4, the maximum difference between the calculated and experimental profiles does not exceed 0.5%.

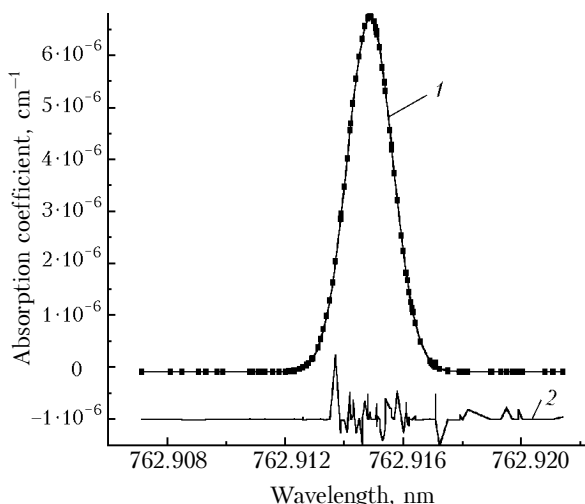


Fig. 4. An example of recorded absorption line profile (curve 1): experiment (■) theoretical Doppler profile (—), and the difference ($k_{\text{exp}} - k_{\text{calc}}$)·50 (curve 2).

Conclusions

The modernization performed of the mirror alignment unit of the optical system and the system for measuring the ratio between the photodetector signals at the entrance into an absorbing gas medium and at the exit from it, enabled us to decrease by almost five times the relative error of measuring the spectral absorption coefficient by the laser spectrometer with the 30-m long cell. When a pulsed laser with the discretely tunable from pulse-to-pulse wavelength is used, $\Delta k/k \sim 4 \cdot 10^{-3}$ at $k \sim 7 \cdot 10^{-6} \text{ cm}^{-1}$.

Acknowledgments

This work was accomplished within the framework of the Program No. 2.10 of the Division of Physical Sciences of the Russian Academy of Sciences and was partly supported by the Russian Foundation for Basic Research (Grant No. 01-5-65152a) and the task-oriented Complex Program "Atmosfera."

References

1. Yu.N. Ponomarev and I.S. Tyryshkin, *Atmos. Oceanic Opt.* **6**, No. 6, 224–228 (1993). Yu.N. Ponomarev and I.S. Tyryshkin, in: *Regional Monitoring of the Atmosphere. Part 3. Unique Measurement Complexes*, ed. by M.V. Kabanov (Nauka, Novosibirsk, 1998), 237 pp.
2. M. Carleer, A. Jenouvrier, A.C. Vandaele, P.F. Bernath, M.-F. Merienne, R. Colin, N.F. Zobov, O.L. Polyansky, J. Tennyson, and S.A. Savin, *J. Chem. Phys.* **111**, No. 6, 2444–2450 (1999).
3. J. Ballard, K. Strong, J.J. Remedios, M. Page, and W.B. Johnston, *J. Quant. Spectrosc. Radiat. Transfer* **52**, No. 5, 677–691 (1994).
4. P. Horowitz and W. Hill, *The Art of Electronics* (Cambridge University Press, 1989).
5. B.G. Fedorkov and V.A. Telets, *DAC and ADC Chips: Functioning, Parameters, Applications* (Energoatomizdat, Moscow, 1990), 354 pp.
6. *1996 Designer's Reference Manual* (MAXIM integrated products, 1996), 413 pp.
7. I.S. Tyryshkin, Yu.N. Ponomarev, A.D. Bykov, B.A. Voronin, O.V. Naumenko, V.N. Saveliev, and L.N. Sinitsa, *Atmos. Oceanic Opt.* **12**, No. 9, 792–795 (1999).
8. E.G. Barskaya and I.L. Kuzovaya, *Opt. Mekh. Promst.*, No. 6, 61–62 (1972).